Pseudopotential inversion scheme

Jeffrey R. Gardner* and N. A. W. Holzwarth
Department of Physics, Wake Forest University, Winston-Salem, North Carolina 27109
(Received 20 December 1985)

A method is described for deriving all-electron valence wave functions, having the correct nodal behavior, from the knowledge of the self-consistent nodeless pseudo-wave-functions. The method is tested for several atoms throughout the Periodic Table. The resulting "inverted" wave functions compare closely with the corresponding all-electron frozen-core wave functions, with deviations less than 1%. The method can be extended for use in molecular and solid calculations.

Pseudopotential techniques[1] have proven to be invaluable tools for self-consistent local-density calculations of the electronic structure of solids and molecules. Their use enables accurate evaluation of the valence electron densities and energies. However, within the pseudopotential formalism, information concerning the core region of each atomic site is lost. This core information is important for relating calculated electronic structures to results from various experimental probes, such as nuclear magnetic resonance (NMR), or x-ray and other high-energy spectroscopies. In addition, the core information is important for refining the calculation.

In the original formulation of pseudopotential theory,[2] based on the orthogonalized-plane-wave method of electronic structure calculations,[3] core information could be approximated by orthogonalizing the pseudo-wavefunction to the core wave functions. However, the more recent "first-principles" or "norm-conserving" pseudopotential formulations[1,4,5] promise to approach the accuracy of all-electron frozen-core calculations in determining the valence electron energies and their wave functions in the valence region. Consequently, it should be possible to "invert" the results of a self-consistent first-principles pseudopotential calculation in order to directly retrieve results analogous to those obtainable from an all-electron frozen-core calculation. In this paper, we report a simple scheme developed for this inversion process. The scheme is tested for atomic calculations so that we can make a detailed comparison of the inverted pseudopotential and all-electron results. The comparison is very encouraging for the possibility of implementing the scheme in solids and molecules, and also yields additional insight into the accuracy of the first-principles pseudopotentials themselves. For simplicity, we confine our attention to a nonrelativistic and spherically symmetric (average multiplet) treatment of the atom.

The basis of this work is a self-consistent solution of the one-electron Schrödinger equation within the local density approximation[6] and within the "frozen-core"[7] approximation. In an all-electron treatment, the effective electronic potential[6] for an atom having atomic number Z is given by

$$V(\mathbf{r})=-\frac{Ze^2}{r}+e^2\int d^3r'\frac{\rho_c^{\mathrm{FC}}(r')}{|\mathbf{r}-\mathbf{r}'|}+e^2\int d^3r'\frac{\rho_v^{\mathrm{FC}}(r')}{|\mathbf{r}-\mathbf{r}'|}+V_{\mathrm{xc}}[\rho_c^{\mathrm{FC}}(r)+\rho_v^{\mathrm{FC}}(r)]\ . \tag{1}$$

Here, e is the charge of an electron, and $\rho_c^{\mathrm{FC}}(r)$ and $\rho_v^{\mathrm{FC}}(r)$ denote the spherically symmetric density distribution of the frozen-core states and of the valence states, respectively. V_{xc} denotes the exchange-correlation functional which we have taken to be that of Hedin and Lundqvist.[8] The solutions to the radial Schrödinger equation are the valence radial wave functions $\Psi_{nl}^{\mathrm{FC}}(r)$ and their eigenvalues E_{nl}^{FC}. Self-consistency means that the valence density $\rho_v^{\mathrm{FC}}(r)$ that appears on the left-hand side of Eq. (1) is related to the valence states nl, having occupancy w_{nl}, according to

$$\rho_v^{\mathrm{FC}}(r)=\sum_{\substack{nl\\(\text{valence states})}} w_{nl}\frac{|\Psi_{nl}^{\mathrm{FC}}(r)|^2}{4\pi}\ . \tag{2}$$

A pseudopotential treatment[1,4,5] can be described operationally as follows. First, the ionic Coulomb potential in Eq. (1),

$$V_{\mathrm{ion}}^{\mathrm{FC}}(\mathbf{r})=-\frac{Ze^2}{r}+e^2\int d^3r'\frac{\rho_c^{\mathrm{FC}}(r')}{|\mathbf{r}-\mathbf{r}'|}\ , \tag{3}$$

is replaced by l-dependent pseudopotentials:

$$V_{\mathrm{ion}}^{\mathrm{ps}}(\mathbf{r})=\sum_l \Phi_l(r)P_l(\hat{\mathbf{r}})\ , \tag{4}$$

where $\Phi_l(r)$ denotes a smooth radial function representing the ionic pseudopotential for valence states of orbital angular momentum l; P_l denotes the projection operator. Secondly, the valence pseudodensity $\rho_v^{\mathrm{ps}}(r)$ replaces $\rho_v^{\mathrm{FC}}(r)$ in Eq. (1) for both the Coulomb repulsion and exchange-correlation contributions. Finally, the frozen-core density $\rho_c^{\mathrm{FC}}(r)$ in the V_{xc} term of Eq. (1) is approximated by a smooth function $\rho_c^a(r)$, following the approach of Louie *et al.*[9] The self-consistent valence pseudodensity $\rho_v^{\mathrm{ps}}(r)$ is related to the nodeless pseudo-wave-functions $\Psi_{nl}^{\mathrm{ps}}(r)$ having valence eigenenergies E_{nl}^{ps}, according to the self-consistency condition analogous to Eq. (2). For "norm-conserving" pseudopotentials,[4,5] the E_{nl}^{ps} closely approximate those of the frozen-core all-electron calculations[4,5]

$$E_{nl}^{\mathrm{ps}}\approx E_{nl}\ . \tag{5}$$

In addition, each pseudo-wave-function closely matches the frozen-core all-electron wave function in the valence region[4,5]

$$\Psi_{nl}^{\mathrm{ps}}(r)\approx\Psi_{nl}^{\mathrm{FC}}(r),\quad r\geq R_l \tag{6}$$

for a pseudopotential radius R_l, chosen to lie close to the last peak of the frozen core all-electron wave function $\Psi_{nl}^{\mathrm{FC}}(r)$. Typically, R_l is chosen so that the pseudopotential functions $\Phi_l(r)$ and $\Psi_{nl}^{\mathrm{ps}}(r)$ are sufficiently smooth for the particular application. A further equality is imposed for norm-conserving pseudopotentials:[4,5]

$$\int_0^{R_l} |\Psi_{nl}^{\mathrm{ps}}(r)|^2 r^2 dr \approx \int_0^{R_l} |\Psi_{nl}^{\mathrm{FC}}(r)|^2 r^2 dr \ . \tag{7}$$

The problem of pseudopotential inversion starts with the results of a self-consistent pseudopotential calculation, including the valence pseudo-wave-functions $\Psi_{nl}^{\mathrm{ps}}(r)$ and their corresponding energies E_{nl}^{ps} and density $\rho_v^{\mathrm{ps}}(r)$, as well as the frozen-core density $\rho_c^{\mathrm{FC}}(r)$. From these results, one would like to determine the inverted all-electron valence density $\rho_v^I(r)$ and valence wave functions $\Psi_{nl}^I(r)$. The inverted wave functions are assumed to be good approximations to the all-electron frozen-core results and are forced to replace them in the right-hand sides of equalities (5)—(7) and to be consistent with Eqs. (1) and (2). From Eqs. (6) and (7), the inverted wave functions $\Psi_{nl}^I(r)$ and corresponding Coulomb potentials are determined from the pseudopotential results for $r > R_l$. Therefore the entire inversion calculation is confined to the core region $0 < r < R_M$ (where R_M is the largest of all the R_l). In principle, the inversion could be carried out by inward integration, starting with the known values at R_l and proceeding toward the origin. However, an analysis of the error propagation of such a scheme showed it to be numerically unstable. Therefore, we adopted an algorithm based on outward numerical integration starting at the origin. Since the screening potential is not entirely known in this region, this scheme is necessarily an iterative one.

Denoting by $\rho_v^{(i)}(r)$ the ith approximation to the valence density, we calculate the corresponding effective potential according to Eq. (1). Then, we numerically integrate the Schrödinger equation for this effective potential for each of the valence states nl, using the eigenenergies from the pseudopotential calculations according to Eq. (5). The numerical integration is accomplished by integrating the radial equation outward from $r=0$ using the Noumerov algorithm.[10] The initial values for the integration are known up to normalization from the asymptotic behavior of the equation for $r \to 0$. This determines the unnormalized wave function for $0 < r < R_l$. For $r > R_l$, $\Psi_{nl}^{(i)}(r) \equiv \Psi_{nl}^{\mathrm{ps}}(r)$ for each iteration so that using Eq. (7), the wave function can be correctly normalized. The results of the numerical integration are new approximations to the valence wave functions, from which we can determine $\rho_v^{(i+1)}(r)$. In practice, in order to avoid numerical instability, for the $(i+1)$th iteration $\rho_v^{(i+1)}(r)$ is fractionally mixed with $\rho_v^{(i)}(r)$. The process is continued until convergence is achieved. We have obtained rapid convergence using the starting iteration

$$\rho_v^{(0)}(r) = \rho_v^{\mathrm{ps}}(r) \ . \tag{8}$$

In general, the inverted wave function will suffer a discontinuity at R_l. The magnitude of the discontinuity

$$\Delta_{nl} \equiv R_l[\Psi_{nl}^I(R_l^-) - \Psi_{nl}^{\mathrm{ps}}(R_l)] \tag{9}$$

for the converged wave function is generally small; its smallness is a measure of the success of the inversion process.

Another quantity of interest and measure of accuracy is the total electronic energy.[1,7] We have calculated a total valence energy in the form

$$E_T = \sum_{\substack{nl \\ \text{(valence states)}}} w_{nl} E_{nl}^I - \tfrac{1}{2} \int d^3r d^3r' \frac{\rho_v^I(r)\rho_v^I(r')}{|\mathbf{r}-\mathbf{r}'|} - \int d^3r \rho_v^I(r) V_{\mathrm{xc}}(\rho_c^{\mathrm{FC}}(r) + \rho_v^I(r)) + E_{\mathrm{xc}}(\rho_c^{\mathrm{FC}} + \rho_v^I) - E_{\mathrm{xc}}(\rho_c^{\mathrm{FC}}) \ , \tag{10}$$

where E_{xc} denotes the exchange-correlation energy functional.[8] Since we are working within the frozen-core approximation, the constant-core contributions[7] have not been included. $E_{\mathrm{xc}}(\rho_c^{\mathrm{FC}})$ has been subtracted in order to facilitate comparison with the pseudopotential total energies which can be calculated using the same form, but replacing the frozen-core density $\rho_c^{\mathrm{FC}}(r)$ with the approximate core density[9] $\rho_c^a(r)$.

In the present work, we have used the norm-conserving pseudopotential formalism of Kerker,[5] which uses R_l as a matching radius. We have studied the inversion of pseudo-wave-functions for a series of atoms throughout the Periodic Table. The convergence of the iteration scheme was very rapid: On the order of 100 iterations were needed for all the materials studied. The results are of two general types, depending upon the accuracy of Eqs. (5)—(7). The first type of result is obtained when Eqs. (5)—(7) are essentially exact, using the pseudo-wave-functions determined for the atom in the same configuration as that used to construct the pseudopotential.[5] In this case, the errors are due solely to numerical errors in integration. For all the materials studied in this case, the discontinuity errors [Eq. (9)] were less than 5×10^{-5} bohr$^{-1/2}$ and the difference between the inverted and all-electron frozen-core total energies were less than 0.0005 Ry, as expected from the numerical methods.

The second type of result was obtained when Eqs. (5)—(7) were only approximately satisfied. Operationally, this occurs when the pseudo-wave-functions are determined for an atom having a configuration that is different from the one used to construct the pseudopotential.[5] Since this case is of more general interest, the figures and tables pertain to it. Figures 1 and 2 illustrate the iteration process for the inverted valence charge density and the corresponding Coulomb potential. In these figures, the starting values are shown with dotted curves; the first iteration results are shown with dashed curves; and the final iteration is indistinguishable from the exact frozen-core result, shown with the solid line. The effects of the discontinuities at the pseudopotential radii R_l are not visi-

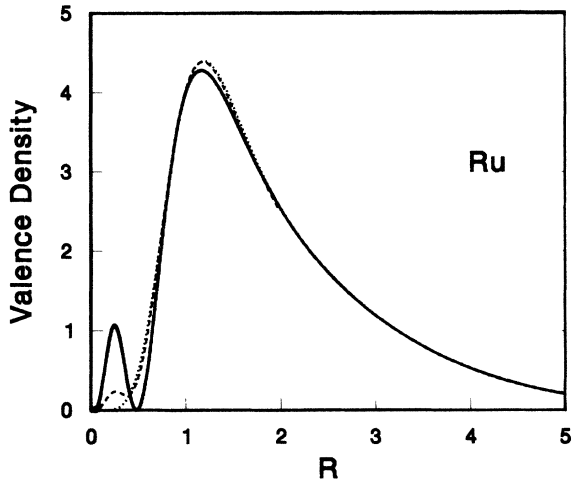

FIG. 1. Radial valence densities $[4\pi r^2\rho(r)]$ in units of electrons/bohr plotted as a function of radius r in bohr units. The atom is Ru, calculated using pseudopotential parameters listed in Table I. Dotted curve shows pseudopotential density (starting iteration); dashed curve shows first iteration of inverted density; dash-dot curve (not resolved) shows converged inverted density; solid curve shows all-electron frozen-core density.

ble on the scale of these figures.

In order to make a more detailed comparison of the inverted results with the exact frozen-core results, we have plotted the density differences:

$$\Delta\rho(r)\equiv\rho_v^I(r)-\rho_v^{\mathrm{FC}}(r) \tag{11}$$

in Fig. 3 for two different pseudopotentials. For $r>R_l$,

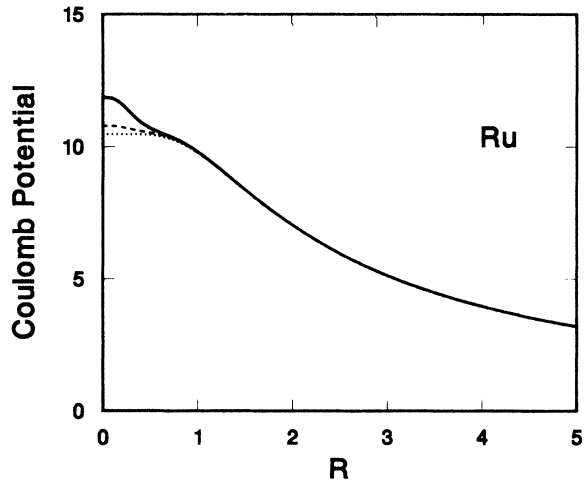

FIG. 2. Coulomb repulsion potential for valence densities given in Fig. 1 in units of rydbergs, plotted as a function of radius r in bohr units. The atom is Ru, calculated using pseudopotential parameters listed in Table I. Dotted curve shows pseudopotential repulsion (starting iteration); dashed curve shows first iteration of inverted repulsion; dash-dot curve (not resolved) shows converged inverted repulsion; solid curve shows all-electron frozen-core repulsive potential.

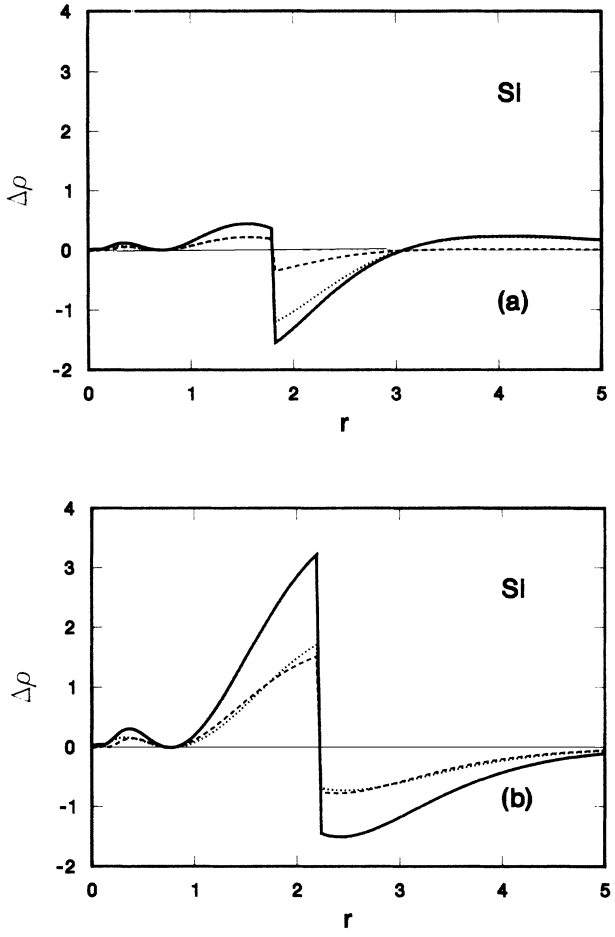

FIG. 3. Radial valence density deviations $[4\pi r^2\Delta\rho(r)]$, where $\Delta\rho(r)$ is given in Eq. (11), in units of 10^{-3} electrons/bohr plotted as a function of radius r in bohr units. The atom is Si with $R_{3s}=R_{3p}=R_l$, using $R_l=1.8$ bohr in (a) and $R_l=2.2$ bohr in (b). Dashed curve shows $3s$ contributions, dotted curve shows $3p$ contributions, and solid curve shows the total density deviations.

the deviation is directly due to the pseudodensity error: $\rho_v^{\mathrm{ps}}(r)$-$\rho_v^{\mathrm{FC}}(r)$. For $r<R_l$, the deviation is due to the inverted density error, the discontinuity at R_l being prominent in these plots. The results illustrate the sensitivity of the inversion results to the accuracy of the original pseudo-wave-functions, those of Fig. 3(a) being slightly more accurate than those of Fig. 3(b). It is interesting to note that in Fig. 3(a), the maximum deviation is smaller and occurs in the pseudopotential region $r>R_l$, while in Fig. 3(b), it is larger and occurs in the inversion region $0<r<R_l$. In Fig. 3(a), the pseudodensity deviation has both signs, which has a cancellation effect on the inversion error, while in Fig. 3(b) the pseudodensity deviation has only one sign, which has an accumulative effect on the inversion error.

Results for a variety of different atoms are listed in Table I. The pseudopotential parameters are given in column 1. The configuration of calculation is given in column 2. In column 3, the values of the wave-function

TABLE I. Survey of atomic results.

Pseudopotential parameters	Configuration of calculation	Inversion error[a] Δ_{nl}	One-electron energies[b] E_{nl}^{ps}	δE		Total energies[c] E_T	ΔE_T
C($2s^2 2p^2$)	$2s^1 2p^3$				inv	−10.2012	0.6018
$R_{2s}=1.4$ bohr		$\Delta_{2s}=1\times10^{-4}$	$E_{2s}=-1.0396$	+0.0007	frz	−10.1985	0.6045
$R_{2p}=1.4$ bohr		$\Delta_{2p}=3\times10^{-4}$	$E_{2p}=-0.4347$	−0.0003	psd	−10.2014	0.6017
Si($3s^2 3p^2$)	$3s^1 3p^3$				inv	−7.1207	0.4973
$R_{3s}=1.8$ bohr		$\Delta_{3s}=4\times10^{-4}$	$E_{3s}=-0.8575$	+0.0002	frz	−7.1219	0.4960
$R_{3p}=1.8$ bohr		$\Delta_{3p}=4\times10^{-4}$	$E_{3p}=-0.3552$	+0.0002	psd	−7.0817	0.4949
Si($3s^2 3p^2$)	$3s^1 3p^3$				inv	−7.1241	0.4939
$R_{3s}=2.2$ bohr		$\Delta_{3s}=2\times10^{-3}$	$E_{3s}=-0.8584$	−0.0007	frz	−7.1219	0.4960
$R_{3p}=2.2$ bohr		$\Delta_{3p}=6\times10^{-4}$	$E_{3p}=-0.3552$	+0.0001	psd	−7.0906	0.4956
K($4s^1 4p^0$)	$4s^{.5} 4p^{.5}$				inv	−0.2709	0.0591
$R_{4s}=3.4$ bohr		$\Delta_{4s}=6\times10^{-4}$	$E_{4s}=-0.2096$	+0.0001	frz	−0.2710	0.0589
$R_{4p}=4.0$ bohr		$\Delta_{4p}=8\times10^{-4}$	$E_{4p}=-0.0901$	+0.0001	psd	−0.2649	0.0565
Fe($4s^2 4p^0 3d^6$)	$4s^1 4p^0 3d^7$				inv	−43.8330	−0.0496[d]
$R_{4s}=2.0$ bohr		$\Delta_{4s}=2\times10^{-3}$	$E_{4s}=-0.3314$	−0.0028	frz	−43.8610	−0.0771
$R_{4p}=2.2$ bohr		$\Delta_{4p}=3\times10^{-3}$	$E_{4p}=-0.0791$	−0.0016	psd	−42.2137	−0.0767
$R_{3d}=1.8$ bohr		$\Delta_{3d}=3\times10^{-5}$	$E_{3d}=-0.3011$	+0.0062			
Mo($5s^1 5p^0 4d^5$)	$5s^{1.35} 5p^0 4d^{4.65}$				inv	−16.2899	0.0010
$R_{5s}=3.0$ bohr		$\Delta_{5s}=3\times10^{-4}$	$E_{5s}=-0.3220$	+0.0008	frz	−16.2821	0.0090
$R_{5p}=4.0$ bohr		$\Delta_{5p}=4\times10^{-4}$	$E_{5p}=-0.1006$	+0.0006	psd	−16.0776	0.0058
$R_{4d}=1.5$ bohr		$\Delta_{4d}=7\times10^{-4}$	$E_{4d}=-0.3658$	−0.0007			
Ru($5s^1 5p^0 4d^7$)	$5s^2 5p^0 4d^6$				inv	−33.7914	0.1594
$R_{5s}=2.5$ bohr		$\Delta_{5s}=2\times10^{-3}$	$E_{5s}=-0.3817$	+0.0023	frz	−33.7726	0.1787
$R_{5p}=3.0$ bohr		$\Delta_{5p}=2\times10^{-4}$	$E_{5p}=-0.1183$	+0.0017	psd	−33.4005	0.1717
$R_{4d}=2.0$ bohr		$\Delta_{4d}=3\times10^{-3}$	$E_{4d}=-0.6360$	−0.0034			
Hg($6s^2 6p^0$)	$6s^1 6p^1$				inv	−1.6138	0.3123
$R_{6s}=2.9$ bohr		$\Delta_{6s}=2\times10^{-3}$	$E_{6s}=-0.5001$	−0.0002	frz	−1.6137	0.3124
$R_{6p}=2.9$ bohr		$\Delta_{6p}=5\times10^{-4}$	$E_{6p}=-0.1761$	+0.0003	psd	−1.5722	0.3036

[a] Δ_{nl} [Eq. (9)] given in units of $(\text{bohr})^{-1/2}$.
[b] Energies given in rydbergs; $\delta E = E_{nl}^{ps} - E_{nl}^{FC}$.
[c] Energies given in rydbergs; $\Delta E_T = E_T$(configuration in column 2) $- E_T$[configuration in column 1 (ground state)]; inv, frz, and psd denote inverted, frozen core, and pseudopotential total energies [Eq. (10)], respectively.
[d] Unphysical result for Fe due to average multiplet treatment.

discontinuities at R_l [Eq. (9)] are listed. For most of the materials studied, this discontinuity is in the range of 10^{-4}–10^{-3}. In order to quantify the quality of the pseudopotential, the one-electron pseudopotential energies and their discrepancies with respect to the frozen-core results are given in columns 4 and 5, respectively.[1,4,5] With the exception of the results for Fe and Ru, for which the pseudopotentials are of lower quality, the one-electron energies had errors less than 0.001 Ry. In columns 6 and 7, the total valence energies as calculated using Eq. (10) and the energy differences with respect to the ground state are listed. Results for Mo in the $5s^{1.35}4d^{4.65}$ configuration were included in order to verify our frozen-core total energies with those published by von Barth *et al.*[7] Again, with the exception of Fe and Ru, the inverted total energy results are within 0.003 Ry of the frozen-core results. The pseudopotential energies are also listed for comparison.[1] It is interesting to note that although the "absolute" values of the energies calculated from Eq. (10) cannot be expected to be the same for the frozen-core and pseudopotential calculations, the pseudopotential total energy differences between the excited and ground configurations agree quite well with both the frozen-core and inverted results.[1] It is somewhat disappointing that the inverted total energy differences are not reliably more in agreement with the frozen-core results than are the pseudopotential total energy differences. This is a further illustration of the point that the inversion results are intimately tied to the accuracy of the starting pseudo-wave-functions.

In conclusion, we have demonstrated an efficient scheme for retrieving core information from a self-consistent pseudopotential calculation. This scheme has been demonstrated for atoms, but can be extended for use in solids and molecules, potentially extending the power

of the pseudopotential approach. We found that the accuracy of the inversion is tied to the accuracy of pseudo-wave-functions. In order to improve the accuracy of both, one might try to revise some of the existing schemes for constructing pseudopotentials, in order to make them more configuration independent. However, for many applications, the present accuracy is quite good; the magnitude of the errors being comparable to that of the errors of the frozen-core approximation[7] and of the local-density approximation itself.[6–8]

This work was supported by National Science Foundation Grant No. DMR-85-01022.

*Present address: Woodberry Forest School, P.O. Box 46, Woodberry Forest, VA 22989.

[1]M. L. Cohen, Am. J. Phys. **51**, 695 (1984); M. T. Yin and M. L. Cohen, Phys. Rev. **25**, 7403 (1982); M. L. Cohen and J. R. Chelikowsky, in *Handbook on Semiconductors,* edited by T. S. Moss (North-Holland, Amsterdam, 1982), Vol. I, p. 219; S. G. Louie, K.-M. Ho, and M. L. Cohen, Phys. Rev. B **19**, 1774 (1979).

[2]J. C. Phillips and L. Kleinman, Phys. Rev. **116**, 287 (1959).

[3]C. Herring, Phys. Rev. **57**, 1169 (1940).

[4]D. R. Hamann, M. Schluter, and C. Chiang, Phys. Rev. Lett. **43**, 1494 (1979).

[5]G. P. Kerker, J. Phys. C **13**, L189 (1980).

[6]P. Hohenberg and W. Kohn, Phys. Rev. **136**, B864 (1964); W. Kohn and L. J. Sham, Phys. Rev. **140**, A1333 (1965).

[7]U. von Barth and C. D. Gelatt, Phys. Rev. B **21**, 2222 (1980).

[8]L. Hedin and B. I. Lundqvist, J. Phys. C **4**, 2064 (1971).

[9]S. G. Louie, S. Froyen, and M. L. Cohen, Phys. Rev. B **26**, 1738 (1982).

[10]D. R. Hartree, *Numerical Analysis,* 2nd ed. (Oxford University Press, London, 1958), p. 142.